

UNCLASSIFIED

**Defense Technical Information Center
Compilation Part Notice**

ADP014258

TITLE: Characterization of Metal-Oxide Nanoparticles: Synthesis and Dispersion in Polymeric Coatings

DISTRIBUTION: Approved for public release, distribution unlimited

This paper is part of the following report:

TITLE: Materials Research Society Symposium Proceedings Volume 740
Held in Boston, Massachusetts on December 2-6, 2002. Nanomaterials for Structural Applications

To order the complete compilation report, use: ADA417952

The component part is provided here to allow users access to individually authored sections of proceedings, annals, symposia, etc. However, the component should be considered within the context of the overall compilation report and not as a stand-alone technical report.

The following component part numbers comprise the compilation report:
ADP014237 thru ADP014305

UNCLASSIFIED

Characterization of Metal-Oxide Nanoparticles: Synthesis and Dispersion in Polymeric Coatings

Li-Piin Sung, Stephanie Scierka, Mana Baghai-Anaraki, and Derek L. Ho
National Institute of Standards and Technology
Gaithersburg, MD 20899, U.S.A.

ABSTRACT

Metal-oxide nanoparticles can be used to optimize UV absorption and to enhance the stiffness, toughness, and probably the service life of polymeric materials. Characterization of the nano- and microstructure dispersion of particles is necessary to optimize the structure-property relationships. Characterizations of both TiO_2 particles dispersed in an acrylic-urethane matrix and TiO_2 nanostructured films obtained through sol-gel synthesis are discussed. Experimental methods include microscopy (confocal, AFM) and small angle neutron scattering (SANS). Results from SANS experiments, which yield information about the cluster size of the nano- TiO_2 particles and the spatial dispersion in various nanoparticle/polymer samples are presented and compared to the results of microscopy studies.

INTRODUCTION

Metal-oxide particles (or pigments), such as TiO_2 and ZnO , serve many functions in the various polymeric materials. Traditionally, they have been used as pigments to enhance the appearance and improve the durability of polymeric products, and usually they have been considered to be inert. As nanosized particles, these materials exhibit broad band UV absorption, a benefit that currently has been exploited only in sunscreen applications. Also, the addition of nanoparticles would likely enhance the stiffness, toughness, and service life of polymeric materials, for example, in applications in which mar resistance is important. Optimizing the material properties of metal-oxide nanoparticle/polymer composites, the microstructure and dispersion (sizes and spatial distribution) of nanoparticles must be characterized as a function of different process conditions.

In this project, non-destructive characterization methods, such as small angle neutron scattering (SANS), laser scanning confocal microscopy (LSCM) and atomic force microscopy (AFM), were used to determine the spatial dispersion of nano-pigments (mainly TiO_2) in polymeric binders and in nanostructured TiO_2 samples prepared using a sol-gel method. For the nanoparticle/polymer composites, particle sizes, dispersion time, and pigment concentration were varied. The results will be compared to those obtained via transmission electron microscopy (TEM).

EXPERIMENTAL DETAILS*

* Certain instruments or materials are identified in this paper in order to adequately specify experimental details. In no case does it imply endorsement by NIST or imply that it is necessarily the best product for the experimental procedure.

Materials

The particulate materials used in this study included: pigmentary TiO₂ (CR-800, Kerr McGee) and nano-TiO₂ (P-25, Degussa). The average diameters (provided by manufacturers) of these particles were 190 nm and 25 nm for CR-800 and P-25, respectively. TiO₂ particle/polymer films were prepared by dispersing TiO₂ into an acrylic-urethane binder by hand or using a dispermat mixer (BYK Gardener) and then applying the mixture onto release paper using a draw-down blade. The films were cured at room temperature for at least one day. Various particle concentrations and processing conditions were used to examine and improve the dispersion. Additionally, to improve organic compatibility for the dispersion, P-25 was silanized using octyltrichlorosilane (OTS) to obtain a nanoparticle slurry [1]. Nanostructured TiO₂ films obtained using sol-gel synthesis were also studied. Two types of sol-gel processes were used: hydrolysis (sol-product) [2] and condensation (gel-product) [3]. Reactants include titanium tetraisopropoxide (Aldrich), isopropanol (Mallinkrodt), nitric acid (JT Baker), and deionized water. Different sol-gel processing conditions, such as TiO₂ concentration and sintering temperature were examined.

Microscopy

Laser scanning confocal microscope (LSCM)

A Zeiss model LSM510 laser scanning confocal microscope (LSCM) was used to characterize dispersion and microstructure in the film samples. An oil immersion objective (100 \times /1.3) was used to minimize the scattered intensity from the polymer-air surface. The scanning area of each confocal micrograph was about 18.4 μm \times 18.4 μm at 0.18 μm /pixel, with a scanning time of 8 s/frame. The calculated transverse and depth resolutions (point-to-point spread function) for an objective with a numerical aperture (N.A.) of 1.3 are 155 nm and 286 nm, respectively, for a scanning laser wavelength of 543 nm [4].

Atomic Force Microscopy (AFM)

A Dimension 3100 Scanning Probe Microscope with Nanoscope IIIa controller from Digital Instruments was operated in tapping mode to characterize the surface morphology (nanostructure) of TiO₂ films. Silicon microcantilever probes (TESP, Digital Instruments) were used. Topographic and phase images were obtained simultaneously using a resonance frequency of approximately 300 kHz for the probe oscillation and a free-oscillation amplitude of 62 nm \pm 2 nm. The set-point ratio (the ratio of set point amplitude to the free amplitude) ranged from 0.60 to 0.80.

Small angle neutron scattering (SANS)

Small angle neutron scattering measurements were performed at the NIST Center for Neutron Research using the 30 m SANS instrument with a combination of various wavelengths and a special focusing neutron optics-device [5] to achieve a wide range of size scale from 1 nm to 1 μm . After standard calibrations and accounting for the sample transmission and film thickness, two-dimensional scattering images were averaged azimuthally to produce a one-dimensional absolute scattering intensity curve as a function of the scattering wave vector q . Here, $q = 4\pi\sin(\theta/2)/\lambda$, where θ is the scattering angle and λ is the wavelength. Because TiO₂ has a higher neutron scattering cross section than the polymeric binder, the neutron scattering intensity is proportional to the differences in TiO₂ concentration within the sample.

The total coherent scattered intensity (from micro-domain), $I(q)$, can be modeled as:

$$I(q) = I(0) P(q) S(q) \quad (1)$$

where $P(q)$ is the single particle form factor and $S(q)$ is the structure factor [6]. $I(0)$ is proportional to the scattering amplitude (scattering contrast between the particles and the polymer matrix) and the concentration of particles. The form factor $P(q)$ is characteristic of the size and shape of the particles. The structure factor, $S(q)$, is related to the correlation function describing the radial distribution function between particles or micro-domains. A peak in the scattering profile at a scattering wave vector q indicates the existence of micro-domains with a characteristic average length $d = 2\pi/q_{\text{peak}}$. The estimated extended uncertainties ($k=2$) in the SANS data presented in this paper are smaller than the size of symbols.

RESULTS AND DISCUSSION

Dispersion of TiO_2 particle in polymeric coatings

Traditionally, transmission electron microscopy (TEM) has been used to measure the particle size of metal oxides before dispersion into polymer resins. In Figure 1, conventional TEM micrographs are shown for the TiO_2 samples used in this study. The images were taken on an FEI CM30 transmission electron microscope equipped with a Noran energy dispersive spectrometer. The images were collected at 300 kV and were recorded on a Gatan Model 679 slow scan CCD camera. The samples were prepared by dipping a carbon-coated grid into the sample powders. No grinding or suspension of the powder was performed. The images clearly show that TEM only provides a rough estimate of the particle size and shows that the oxides aggregate into polydispersed clusters.

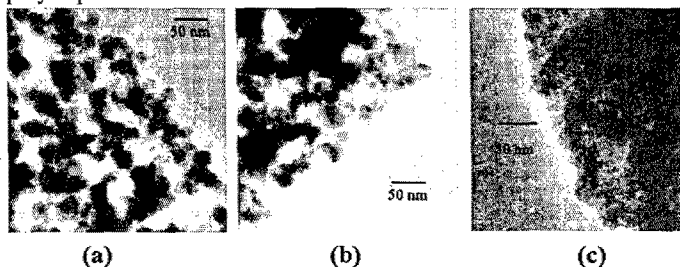


Figure 1. TEM micrographs of TiO_2 samples: (a) P-25, (b) organic silanated treated P-25, and (c) gel product (150 g/L, RT, air-dried).

For the particle/polymer composite films, various TiO_2 particle concentrations and processing conditions were carried out to examine the dispersion of particles in the polymeric binder. In Figures 2a–h, LSCM images are shown for TiO_2 composite films. These micrographs are two dimensional (2D) intensity projections, which consists of a stack of Z- slices with 150 nm thickness increments. Figures 2a–b, films with CR-800 (190 nm diameter) particles are shown for two different concentrations: 1 % vs. 2.5 %. Here, the “%” denotes the particle volume concentration (PVC), calculated as $100 \times (\text{volume of particles} / \text{volume of the sample})$. In Figures 2c–d, films with P-25 (25 nm diameter) are shown for PVC of 1 % and 2.5 %, respectively. For PVC of 2.5 %, changes in distribution are shown in Figures 2e–h for dispermat mixing times of 5 min, 10 min, 20 min, and 40 min, respectively. Note that the scattered intensity from particles is proportional to r^6 , where r is the radius of particle, so that a single nanoparticle of 25 nm is not

visible in the LSCM images. All particles observed in the P-25 samples are thus aggregated clusters. All 1 % PVC samples appear to have slightly poorer dispersion compared to the 2.5 % samples, and the P-25 nanoparticles dispersed poorly in all cases in spite of increasing dispersion times (see Figure 2 e-h.)

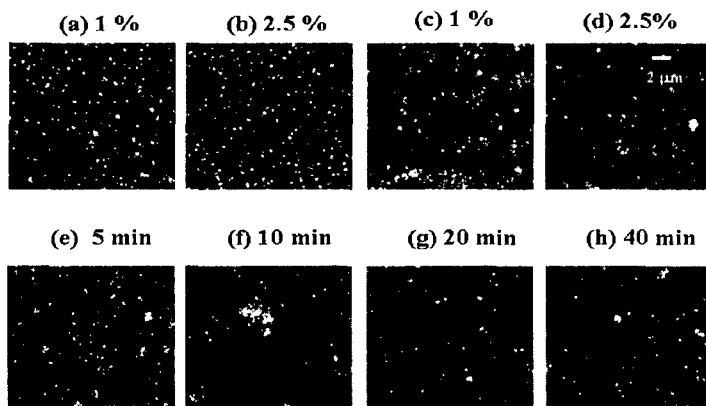


Figure 2. LSCM micrographs of TiO_2 in polymeric binder: (a) and (b) pigmentary TiO_2 particle films. (c) and (d) TiO_2 nanoparticle films; (e)-(h) show TiO_2 nanoparticle (2.5 % PVC) distribution in the polymer films after 5 min to 40 min dispersion times using Dispermat.

Microscopy results represent local and near-surface structures (for example, the probing depth without changing optical contrast is about $8\text{ }\mu\text{m}$ for P-25, 2.5 % PVC samples,) and it is laborious to analyze the particle/cluster sizes from large number of images to obtain sufficient statistics with reasonable resolution. To analyze the dispersion of TiO_2 in the polymeric coatings, SANS was used to characterize the microstructure of the TiO_2 /polymer system (Figure 3). From the intensity profile, $I(q)$, in this measurable q -range, the overall cluster size of the sample containing P-25 particles mixed by hand was found to be similar to that of the sample containing pigmentary particles ($\approx 190\text{ nm}$ diameter) mixed by hand. In general, the particle cluster size in the sample containing organic silanated treated P-25 mixed using a Dispermat mixer is smaller than those samples containing P-25 without treatment, and was much smaller than in the sample mixed by hand. To determine the averaged sizes and spatial distribution of TiO_2 clusters, the general scattering law was applied as indicated in Eq (1), with the assumption that the scatterers (particles/ clusters) are “sufficiently dilute.” In this case, the structure factor $S(q) = 1$ and the form factor $P(q)$ can be generalized using the Guinier approximation [6] for the SANS data in the $q < R_g^{-1}$ region (i.e. for the q values smaller than the turn-over point (q^*) to a plateau region of the log-log plot). The R_g is defined as the radius of gyration of the cluster regardless of the shape of TiO_2 clusters.

However, most of the intensity profiles shown in Figure 3 do not show the clear turn-over plateau region, thus the averaged sizes can not be determined accurately. Nevertheless, we can estimate the average size, $R_g > 21\text{ nm}$ for the sample containing organic silanated treated P-25 /mixed using Dispermat and $R_g > 31\text{ nm}$ for the sample without treatment. Current work aimed to improve dispersion using surfactants and other treatments will be combined with SANS, xray

scattering measurements in the lower q region to quantitatively characterize the dispersion of nano-TiO₂ particles in the polymeric coatings.

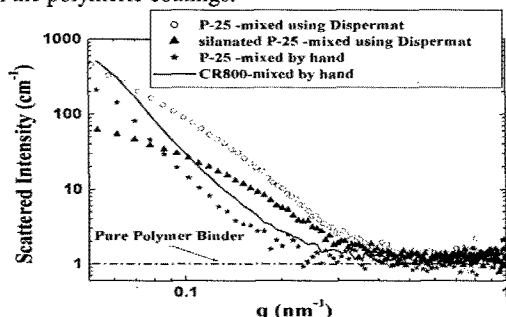


Figure 3. SANS measurements of nano-particles in polymeric binder under different processing conditions. SANS results on the pigmentary particle (CR800) and pure polymeric binder are also shown as reference. The PVC of TiO₂ was 2.5 % in all samples.

TiO₂ network nanostructures prepared through sol-gel synthesis

In addition to using commercially available nano-TiO₂ particles, various sizes of nano-TiO₂ network nanostructures were synthesized by varying and controlling its final particle concentrations and sintering temperatures in sol-gel processing. In Figure 4a, SANS results of the TiO₂ nanostructures prepared using the hydrolysis (sol-product) process are shown for different final particle concentrations. The initial "stock" solution contained titanium isopropoxide, isopropanol, deionized water, and HNO₃ had a calculated concentration of 40 g (TiO₂)/L. Using heat and evaporation, a sol-product (still in a solution form) were prepared with final concentrations of 60 g/L, 124 g/L, and 150 g/L. Similar to the nanoparticle /polymer composite films in the previous section, the R_g of the nanostructure was calculated. Values of $R_g \approx 40 \text{ nm} \pm 2 \text{ nm}$ were determined at the initial concentration (40 g/L) and decreased slowly to $R_g \approx 8 \text{ nm} \pm 0.6 \text{ nm}$ at the final particle concentration (150 g/L). SANS results indicated that the size of the nanostructure decreased as the particle concentration of the solution increased. The SANS result of the final dry film made from 150 g/L solution is also plotted in Figure 4a. The size of film structure is consistent with that of the solution at higher q , however with noticeable increasing intensity at $q < 0.1 \text{ nm}^{-1}$ (a indication of larger structure). The micro/nano-structure of the film was observed using AFM, and an image of the 150 g/L TiO₂ dry film is shown in Figure 4b. The topographic image (left image) shows various network structure with various sizes of clusters and pores. The phase image (right image) reveals uniformly fine structure.

In Figure 4c, SANS results are shown for the TiO₂ network nanostructures prepared using condensation process (gel-product) for various sintering temperatures. All samples are in the dry powder state and have a final TiO₂ particle concentration of 150 g/L in the solution state before the condensation process. Noticeably the intensity profiles of the gel product at sintering temperatures above 300 °C exhibit more complex shape and a broad peak formed at large q , which moves to a lower q value with increasing sintering temperature. The peak in $I(q)$ can be attributed to the presence of homogeneous regions with an averaged diameter $d = 2\pi/q_{\text{peak}}$. The "d" value is estimated to be 12.5 nm at 300 °C and increased to 38.5 nm at 500 °C. This "homogeneous" region is probably related to the pores (between particles) of the network

structure, at which the pore size increases with increasing sintering temperature. In the low q region, the SANS data follows a $I(q) \sim q^{-4}$ scaling law (Porod law [6]), and this scattering profile indicates the formation of larger cluster sizes, in the size which can not be determined in this q range. Overall, the scattering profile of the gel product can be modeled using two length scales. Further analysis of SANS data will be performed and compared to detailed results obtained from TEM and X-ray scattering /diffraction.

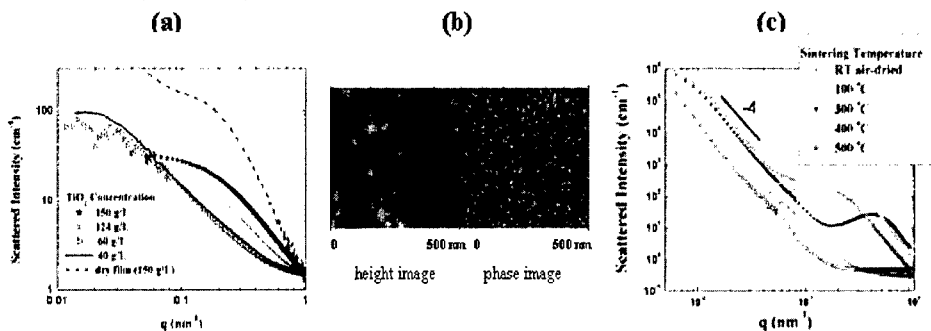


Figure 4. (a) SANS results for TiO₂ sol samples with different concentrations. (b) AFM image (500 nm x 500 nm) of a TiO₂ dry film (150 g/L). (c) SANS results for gel samples prepared using different sintering temperatures.

SUMMARY

We have controlled TiO₂ concentrations and sintering temperatures in the sol-gel process to synthesize various size scales of TiO₂ network nanostructure and improve particle dispersion in the polymeric coating systems by organic silanated treatment. Nanostructure information obtained from SANS allows for designing and implementing techniques to improve the material properties. In combination with microscopic data and modeling of SANS data, the neutron scattering is a powerful tool for non-destructive characterization of the structure and dispersion of nanoparticle/network systems.

ACKNOWLEDGMENTS

The authors thank Professor Chang-lin Lin and Dr. Shirley Turner for helping with the microstructure characterization using AFM and TEM.

REFERENCE

1. S.E. Berger, G.A. Salensky, US Patent 4,061,503 (1977).
2. B. O'Regan, J. Moser, M. Anderson, M. Gratzel, J. Phys.Chem., **94**, 8720-8726 (1990)
3. Y. Haga, H. An, R. Yosomiya, J. Mat.Sci. **32**, 3183-3188 (1997).
4. T.R. Corle, G.S. Kino, G.S., *Confocal Scanning Optical Microscopy and Related Imaging Systems* (Academic Press 1996).
5. S.M. Choi, J.G. Barker, C.J. Glinka, Y.T. Cheng, P.L. Gammel, J Appl Cryst **33**, 793 (2000).
6. J.S. Higgins, H.C. Benoit, *Polymers and Neutron Scattering* (Clarendon Press: Oxford, UK, 1994).

Nanocomposites: Synthesis and Properties